ICES Journal of Marine Science, 2026, Vol. 83, Issue 10, fsag208
https://doi.org/10.1093/icesjms/fsag208
Original article

Reconstructing age and growth history of wild green turtles using eye lens radiocarbon

Moe Kaida[1], Jun Matsubayashi[2], Satomi Kondo[3], Ichiro Tayasu[4], Noriko Iwai [1,*]

[1]Department of Environment Conservation, Tokyo University of Agriculture and Technology, 3-5-8 Saiwai-cho, Fuchu, Tokyo 183-0054, Japan
[2]Faculty of Marine Science and Technology, Fukui Prefectural University, 1-1 Gakuen-cho, Obama, Fukui 917-0003, Japan
[3]Ogasawara Marine Center, Everlasting Nature of Asia, Byobudani, Chichijima, Ogasawara, Tokyo 100-2101, Japan
[4]Research Institute for Humanity and Nature, 457-4 Motoyama, Kamigamo, Kita-ku, Kyoto 603-8047, Japan
*Corresponding author. Department of Environment Conservation, Tokyo University of Agriculture and Technology, 3-5-8 Saiwai-cho, Fuchu, Tokyo 183-0054, Japan. E-mail: iwain@cc.tuat.ac.jp

Abstract

Accurate estimation of age and lifetime growth in sea turtles has long been constrained by their exceptional longevity and extensive migration. Bomb ^{14}C dating has recently attracted attention as a powerful tool for age estimation in long-lived organisms. However, its application requires tissues that retain a lifelong isotopic record. We focused on the eye lens—an inert, non-metabolic tissue that persists throughout the life of an organism—and applied bomb ^{14}C dating to estimate age and reconstruct growth histories of wild green turtles (*Chelonia mydas*). Eye lenses were collected from 48 individuals obtained through legal turtle fisheries, strandings, and mortality in captivity. Age estimation was conducted for eight females and four males using bomb ^{14}C dating. Each lens was dried and scraped layer-by-layer from the exterior toward the core to obtain $F^{14}C$ measurements representing different body sizes. Using coral-derived $F^{14}C$ reference records encompassing the turtles' foraging range, we inferred birth years from lens core $F^{14}C$ values and determined chronological ages. Inner lens sections consistently exhibited higher $F^{14}C$ values than outer sections, reflecting the expected temporal decline following the bomb peak. The estimated ages ranged from 34.9 to 45.6 years for females and from 29.5 to 48.1 years for males. These results indicate that females and males reach sexual maturity at approximately 31 and 28 years of age, respectively, which is consistent with the results of previous studies. The oldest individuals suggested a minimum lifespan of approximately 48 years. Radiocarbon measurements were obtained from multiple lens layers in three individuals. Using the allometric relationship between lens size and straight carapace length derived from all samples, we estimated the body size at the time each layer was formed and reconstructed individual growth trajectories. The resulting growth curves, including growth rates and asymptotic body sizes, were consistent with estimates from mark–recapture and skeletochronological studies on *C. mydas*. This study suggests that the reptilian eye lens provides a chronologically layered structure that remains stable through time, offering a promising framework for retrospective ecological and life-history reconstruction.

Keywords age estimation, *Chelonia mydas*, growth curve, longevity, Sea turtle

Introduction

Accurate age estimation provides essential data for growth modelling (Chen et al. 2022), recruitment analyses (Catalano and Allen 2010), longevity research (Singaram et al. 2013), and evaluations of sexual maturity (Tsikliras and Stergiou 2015). This information helps us obtain data on population dynamics (Hixon et al. 2014) and informs effective management and conservation strategies. However, determining the age of wild animals, particularly long-lived and wide-ranging species, is sometimes difficult using only conventional approaches such as skeletochronology or mark-recapture studies.

Sea turtles are an iconic group of animals with long lifespans (Kamezaki 2012), for which accurate age estimation is essential for understanding population dynamics. Because sea turtles lack external morphological features that reveal their age, studies have primarily relied on skeletochronology—a conventional technique that involves counting annual growth marks (lines of arrested growth; LAGs) in bones, such as the humerus (Turner Tomaszewicz et al. 2022, Usategui-Martín et al. 2023, Medetian and Miaud 2024). This approach has successfully yielded valuable demographic and age-related data across several sea turtle species (Avens et al. 2015, 2021, Turner Tomaszewicz et al. 2022). Nevertheless, skeletochronology has inherent limitations: endosteal resorption often causes early LAGs to disappear, requiring correction factors; LAG deposition may not consistently follow a strict annual pattern; and tightly spaced outer LAGs become increasingly difficult to distinguish in older individuals (Bjorn-

Received: 4 June 2026. **Revised:** 30 September 2026. **Accepted:** 1 October 2026
© The Author(s) 2026. Published by Oxford University Press on behalf of International Council for the Exploration of the Sea. This is an Open Access article distributed under the terms of the Creative Commons Attribution License (https://creativecommons.org/licenses/by/4.0/), which permits unrestricted reuse, distribution, and reproduction in any medium, provided the original work is properly cited.

Downloaded from academic.oup.com/icesjms/article/83/10/fsag208/9004402 by guest on 01 November 2026

dal et al. 1998, Avens et al. 2015, Usategui-Martín et al. 2023). Consequently, robust novel methods for reliably estimating the absolute age of wild sea turtles remain critically needed to advance life-history inferences and support evidence-based management and conservation.

Bomb ^{14}C dating is a promising alternative to existing age estimation techniques. Radiocarbon (^{14}C) is a naturally occurring radioactive isotope whose atmospheric concentration increased sharply during the mid-20th-century from nuclear weapons tests, creating the "bomb-carbon" spike (Eglinton et al. 2023). This pulse provides a temporal marker for terrestrial organisms (Matsubayashi and Tayasu 2019, Suetsugu et al. 2020). As excess ^{14}C was subsequently absorbed by seawater, similar temporal trajectories formed in the oceans (Andrews et al. 2014, Wu et al. 2021). Although this signal was lagged by approximately 10 years and attenuated due to ocean mixing, age assessment using bomb ^{14}C dating still serves as a viable temporal marker for marine organisms, with a long line of successful applications (Andrews et al. 2013, Christiansen et al. 2016, Shervette et al. 2025). For example, radiocarbon analysis of scute tissue has yielded reliable age estimates for hawksbill turtles, *Eretmochelys imbricata*, with an estimated age at maturity of 18–38 years (Van Houtan et al. 2016). Although this method has not been applied to other sea turtle species, the result suggests that bomb ^{14}C dating of a tissue that retains a lifelong isotopic record can determine the absolute age of sea turtles.

The eye lens has emerged as an ideal tissue for retaining stable chronological isotopic records that capture the dietary and environmental conditions experienced at the time of formation in diverse taxa, including fishes (Wallace et al. 2014), cephalopods (Sakamoto et al. 2023), mammals (Miura et al. 2025), birds (Hasegawa et al. 2025), and amphibians (Shiga et al. 2025). The eye lens is formed at birth in its central part and grows outward in layers throughout life (Horwitz 2003). Therefore, isotope analysis of the core reflects birth conditions and maternal isotopic signatures, whereas outer layers reflect later stages of life. Previous studies used radiocarbon analysis of eye lenses to estimate the absolute ages of long-lived marine fish species (Nielsen et al. 2016, Patterson III et al. 2021), utilizing regional reference radiocarbon chronologies (Andrews et al. 2013, Shervette et al. 2025). Nevertheless, this method has never been applied to sea turtles, probably because it remains unclear whether reptilian eye lenses retain precise and reliable radiocarbon signals over extended periods.

Another useful property of the eye lens is that its size is often proportional to body size across many taxa (Mohamed and Augusteyn 2018, Leifsdóttir and Campana 2023, Shiga et al. 2025). Once validated for a target species, this relationship allows estimation of the body size at which a specific lens section was formed (Matsubayashi et al. 2026). By combining this with time-series radiocarbon age estimation using the eye lens, we can reconstruct the growth histories of wild individuals. Specifically, by estimating the absolute age from each layer and the corresponding body size from lens size, we can reconstruct individual growth trajectories. In sea turtles, a similar approach using humeri has been attempted, where growth histories were reconstructed by relating the widths of lines of arrested growth to body size (Zug et al. 2002, Goshe et al. 2010). However, this method is limited, as the humerus core, formed during early life stages, is often resorbed (Bjorndal et al. 1998, Zug et al. 2002). This issue can be overcome by using non-metabolic tissues, as demonstrated in fishes, where otoliths possess distinct growth increments enabling sequential sampling for retrospective analyses (Smoliński and Gutkowska 2024). However, sea turtle otoliths lack this layered morphology. Using the eye lens structure, it is possible to reconstruct long-term growth trajectories of sea turtles, including early developmental stages.

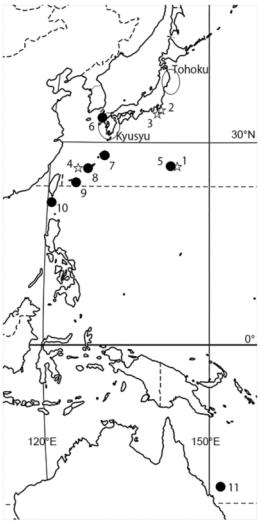


Figure 1 Locations of turtle sampling sites and coral $\Delta^{14}C$ reference sites used in this study. Sampling sites (1–4) are marked with stars (☆), whereas reference sites (5–11) are marked with filled circles (●). 1 and 5: Chichi-jima Island of Ogasawara Islands, 2: Tateyama City, 3: Mikura Island, 4: Kume-jima Island, 6: Iki Island, 7: Kikai Island, 8: Okinawa Island, 9: Ishigaki Island, 10: Nanwan Bay, Taiwan, 11: Masthead Island, Australia.

Here, we investigated whether green turtles (*Chelonia mydas*) retain lifelong radiocarbon signals in their eye lenses and whether these profiles can yield absolute ages for wild individuals. We then applied this method to reconstruct growth histories of field-collected turtles. Although radiocarbon analysis of sea turtle eye lenses requires lethal sampling, this limitation was overcome using samples from the legally managed green turtle fishery in the Ogasawara Islands, Japan.

Materials and methods

Study site and field sampling

Field sampling of green turtles (*C. mydas*) was conducted on Chichi-jima Island in the Ogasawara Islands, Japan (Fig. 1). This species inhabits subtropical and tropical regions worldwide (Seminoff 2002). In the Pacific, its northernmost nesting range includes the Ogasawara and Nansei Islands (Fisheries Agency of Japan 1994). Hatchlings emerge on beaches and enter the open ocean, and as juveniles, they feed on seagrasses and macroalgae in coastal areas (Mortimer 1982, Kameda and Ishihara 2009). Green turtles from the Ogasawara Islands migrate along the Pacific coast of Japan from Okinawa to Tohoku (Fig. 1; Nishizawa et al. 2013, 2014). After maturity, they return to natal waters to

Downloaded from academic.oup.com/icesjms/article/83/10/fsag208/9004402 by guest on 01 November 2026

breed every few years (van Buskirk and Crowder 1994). In the Ogasawara Islands, turtles and mating pairs are observed from March to May, with females nesting on beaches from May to July. On the Ogasawara Islands, a tradition of harvesting green turtles for food consumption exists, and this fishery operates under Tokyo Metropolitan Fishery Adjustment Regulations. Harvesting is limited to adults during mating season, from March to May.

Our field sampling involved adult and juvenile individuals. Samples from both life stages were used to estimate the relationship between body size and eye lens size, whereas only adult samples were used for age estimation. Adult turtles were sampled from 24 March to 18 April, 2024, during traditional local turtle harvests on Chichi-jima Island (Fig. 1). Juvenile specimens were obtained from dead turtles on Mikura Island (10 May to 27 May, 2024), as well as through collaborations with ongoing monitoring projects in Tateyama City, Kume-jima Island, and Chichi-jima Island, Japan (Fig. 1). Much smaller juvenile specimens were obtained from turtles that died in captivity at the Ogasawara Marine Center on Chichi-jima Island. At sampling, biometric data, including straight carapace length (SCL), straight carapace width, body weight, sex (where identifiable), and reproductive status (for adult females, the presence of corpora albicantia, indicating past breeding (Kamezaki 2012)), were recorded for each specimen.

Eye lens pretreatment and dissection

Eye lens dissection was performed following a modified version of Matsubayashi et al. (2026). From each specimen, the eye lenses were extracted using surgical instruments. The eye lenses were subjected to one of three treatments: drying, followed by freezing at −20°C; boiling in water for 3 min, followed by freezing; or immediate freezing without any pretreatment. Drying was conducted by air-drying for 2 days under ambient conditions (mean temperature: 21.4°C; humidity: 79.5% on Chichi-jima Island during the period) or using a hair dryer or silica gel. Before analysis, lenses were thawed and dried at 40°C for 48 h in a drying oven (MOV-212F-PJ, Panasonic Healthcare, Tokyo, Japan). The dried eye lenses were weighed to 0.1 mg using an electronic balance (BM-200; A&D, Tokyo, Japan) to obtain the eye lens weight (ELW). The lenses were incrementally scraped from outer layers inward using forceps under microscopic guidance. Each scraped section was isolated, dried, weighed, and stored separately in pre-labeled microcentrifuge tubes at −20°C until isotopic analysis. Scraping continued until the central portion could no longer be separated into layers (approximately 2–5 mg). For three individuals, the innermost portion disintegrated rather than peeling into layers, and the residual material was analyzed. The innermost samples for these individuals were large (14.5, 16.8, and 18.5 mg, Table 1) compared to those of the other individuals (1.8–5.2 mg, except for one undetermined sample of <8 mg). In two cases, the innermost portion was too small for measurement and was combined with the adjacent layer (2024cc026 and 2024cc028; Table 1).

Radiocarbon measurement

Radiocarbon measurements were conducted on eye lens sections of eight female and four male adult turtles due to sample conditions and practical constraints. For one individual, only the innermost section was measured; for eight individuals, two sections from the inner region—comprising the innermost layer and either the second- or third-innermost layer—were measured; and for three individuals, multiple sections were measured (five samples for one individual and eight samples for each of two individuals) from centre to periphery.

The eye lens sections were graphitized as described previously (Kitagawa et al. 1993). Briefly, the samples were initially freeze-dried and transferred to quartz tubes with CuO and Ag and combusted to CO_2. CO_2 was graphitized with H_2 over an iron catalyst. Targets were prepared at the Research Institute for Humanity and Nature, and ^{14}C concentrations were measured by the Institute of Accelerator Analysis Ltd (Kanagawa, Japan). Radiocarbon results for turtle eye-lens samples are reported as fraction modern, $F^{14}C$, following Reimer et al. (2004). The measured $^{14}C/^{12}C$ ratios were corrected for isotope fractionation using $\delta^{13}C$ values measured by AMS for each sample and normalized to $\delta^{13}C = -25‰$. $F^{14}C$ was calculated as:

$$F^{14}C = A_{SN} \div A_{ON},$$

where A_{SN} is the isotope fractionation-corrected sample activity and A_{ON} is the normalized activity of the modern oxalic acid standard. Analytical uncertainties were estimated from repeated measurements of each sample.

Collection of reference radiocarbon data

Accurate age estimation from measured $F^{14}C$ requires regional reference radiocarbon chronologies (Patterson III et al. 2021). In accordance with previous reports suggesting that the maximum lifespan of green turtles is 75 years (Mayne et al. 2020), we limited our analysis to radiocarbon isotope ratio data from 1950 onward. Reference $\Delta^{14}C$ data were compiled from previously published coral-based radiocarbon data. We restricted our collection of data to coral records because corals are sessile organisms that reflect site-specific radiocarbon levels. We used coral data from the primary habitats and migratory ranges of the sampled green turtles in the western Pacific, including Okinawa Island (Konishi et al. 1981, Mitsuguchi et al. 2016), Ishigaki Island (Mitsuguchi et al. 2004, 2016, Hirabayashi et al. 2017), Kikai Island (Zeng et al. 2024), Iki Island (Morimoto et al. 2004, Mitsuguchi et al. 2016), and Chichi-jima Island (Saito-Kokubu et al. 2019), Japan. We also included radiocarbon records from Taiwan (Nanwan Bay; Ramos et al. 2019) and Australia (Masthead Island; Wu et al. 2021), which provided a continuous radiocarbon chronology from 1950 to 2017. We did not include records from distant regions, such as Guam, Hawaii, and Samoa, since the likelihood of the sampled individuals foraging in those areas is extremely low, based on long-term tagging and tracking field data (Kondo et al. unpublished data), as well as the absence of genetic connection between green turtles in those areas and those in our sampling areas (Dolfo et al. 2023, Jensen et al. 2025). Most published coral records were originally reported as $\Delta^{14}C$. These values were converted to $F^{14}C$ using the independently assigned coral skeletal formation year (x):

$$F^{14}C = \left(1 + \frac{\Delta^{14}C}{1000}\right) \times exp\frac{x - 1950}{8267},$$

This reference dataset was synthesized to develop a representative temporal radiocarbon profile that reflects regional radiocar-

Downloaded from academic.oup.com/icesjms/article/83/10/fsag208/9004402 by guest on 01 November 2026

Table 1 Summary of the 12 green turtles analyzed for age estimation.

		SCL	Innermost section			Second- or third-innermost section			Estimated age		
ID	Sex	(cm)	Size (mg)	$F^{14}C$	SD (10^{-3})	Size (mg)	$F^{14}C$	SD (10^{-3})	Median	Min	Max
2024cc017	F	94.0	4.2	1.149	2.8	37.5	1.073	2.8	42.8	35.9	48.4
2024cc018	F	93.6	18.5	1.112	2.8	–	–	–	37.6	32.6	41.9
2024cc020	F	100.7	1.8	1.129	2.7	14.1	1.104	2.8	35.6	30.9	42.4
2024cc026	F	97.9	2.6	1.127	2.8	5.1	1.121	2.8	34.9	30.3	42.1
2024cc028	F	97.4	3.2	1.131	2.6	14.9	1.108	2.7	36.7	31.8	43.0
2024cc034	F	101.8	5.2	1.156	2.8	9.7	1.142	2.8	45.6	38.0	50.1
2024cc037	F	95.6	2.4	1.138	2.7	6.6	1.083	2.7	39.0	33.4	44.3
2024cc038	F	97.0	2.8	1.140	2.9	6.6	1.127	2.6	39.5	33.8	44.8
Mean (Female)		97.3							39.0	33.3	44.6
2024cc021	M	89.6	14.5	1.121	2.6	–	1.082	2.8	40.4	36.0	48.2
2024cc027	M	89.0	<8.0	1.110	2.8	12.6	1.095	2.7	29.5	24.3	33.5
2024cc033	M	88.6	16.8	1.143	2.7	34.4	1.081	2.7	48.1	42.3	53.7
2024cc036	M	93.2	2.6	1.134	2.7	6.8	1.125	2.7	37.8	32.6	43.5
Mean (Male)		90.1							39.0	33.8	44.7
Mean (All)		94.9							39.0	33.5	44.7

The table lists body size and, for the innermost and second- or third-innermost eye lens sections, eye lens size and $F^{14}C$ values with associated SDs. Eye lens size for the second- or third-innermost section represents the cumulative lens size up to that section, including the innermost section. Ages were calculated based on the formation years of posterior medians with 95% credible intervals conditional on the post-peak branch of the bomb-radiocarbon curve. For the three individuals whose innermost eye lens section was relatively large, 7.6 years were added to the estimated age (see text); these adjusted ages are underlined in the table. SCL: straight carapace length.

bon chronologies that can be used for comparison with $F^{14}C$ profiles of green turtle eye lenses.

Age estimation

We estimated the regional coral-derived $F^{14}C$ reference chronology using a Bayesian latent time-series model implemented in Stan via R 4.4.3 (R core team 2025). The latent reference curve was defined at one-year knots from 1950 to 2017 and coral observation years were entered into the likelihood by linear interpolation between adjacent yearly knots. Let x_t denote the latent regional mean $F^{14}C$ in year t. Temporal smoothness in the reference chronology was imposed using a second-order random-walk prior, so that annual changes in the slope of x_t were regularized by a process standard deviation. Coral measurements were modeled as observations around x_t, with the observation variance given by the sum of analytical uncertainty and an additional residual scatter term. This residual term represents spatial and local variation around the regional mean reference curve. Posterior samples of the reference curve and residual scatter were then propagated into the turtle formation-year estimation. Convergence was checked using standard MCMC diagnostics, including R-hat, effective sample size, divergent transitions, and transitions reaching the maximum tree depth.

For each turtle eye-lens section, the formation year was inferred over the continuous interval from 1950 to 2017, approximated by a 0.1-year grid with trapezoidal integration. A uniform prior density was assigned across this interval. For each candidate year, the likelihood of the measured turtle $F^{14}C$ was evaluated using posterior draws of the linearly interpolated latent coral reference curve. The observation standard deviation combined the analytical uncertainty of the turtle sample, the posterior draw-specific residual scatter estimated from the coral model, and a fixed turtle-specific extra scatter term, which was set to 0 in the present analysis. Grid-point likelihoods were averaged over MCMC draws and then normalized across formation years to obtain the posterior probability distribution. Because a given $F^{14}C$ value can correspond to either the rising or declining limb of the bomb-radiocarbon curve, we also summarized the posterior probability mass for the pre-peak and post-peak branches, defining the peak year separately for each posterior draw of the reference curve.

Growth curve

To estimate body size from ELW, we generated a relationship equation between ELW (mg) and body size using data obtained from all sampled individuals across a wide range of body sizes (SCL: 9.5–101.8 cm). The parameters of the allometric equation, $ELW = f \times (SCL)^{\wedge} g$, where f is the scaling constant and g is the allometric exponent, were estimated using the nls function in R. When both left and right eye lenses were successfully obtained, the mean ELW for each individual was used; if only one lens was available, the value for the single lens was used.

For the three individuals with multiple $F^{14}C$ measurements, individual growth trajectories were constructed. The eye lens size at the formation of each scraped section was defined as the average lens mass before and after scraping (for the innermost section, the remaining lens mass was used). Using the previously derived relationship between eye lens size and body size, the body size at the time of formation of each section was esti-

Downloaded from academic.oup.com/icesjms/article/83/10/fsag208/9004402 by guest on 01 November 2026

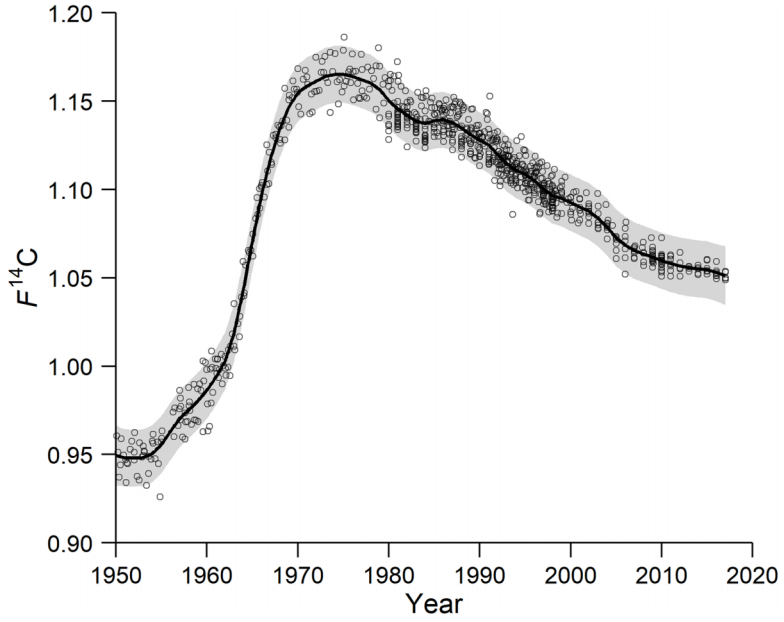


Figure 2 Coral-derived regional $F^{14}C$ reference chronology estimated using a Bayesian latent time-series model. The solid line and shaded band indicate the posterior predictive median and 95% prediction interval, respectively. Open circles represent the observed coral $F^{14}C$ values from 1950 to 2017.

mated. Age estimation for each section was performed using $F^{14}C$ measurements, as described above, and the corresponding estimated body sizes were plotted. The resulting growth trajectories for each individual were fitted with the Von Bertalanffy growth model using the *nls* function in R, and the fitted curves were superimposed.

Results

Field sampling and eye lens dissection

Forty-eight green turtles were sampled (Supplementary Table S1): 26 adults (14 males, 12 females) and 22 juveniles (3 males, 7 females, 12 unknown). The mean SCL was 90.7 cm (SD: ± 2.5, range: 85.8–95.5) and 95.7 cm (± 4.1, range: 85.0–101.8) for adult males and females, respectively. For juveniles, SCL ranged from 9.5 to 55.2 cm. Eye lens dry mass, averaged when both eyes could be sampled, was 66.6 mg (±7.7, range: 53.7–82.7) for adults and 3.3–44 mg for juveniles. Examination of ovarian corpora albicantia confirmed all adult females had reproduced at least once.

Reference radiocarbon data

A dataset for reference $\Delta^{14}C$ data ($n = 880$) was assembled from coral skeletal records at seven locations (Okinawa Island, Ishigaki Island, Kikai Island, Iki Island, and Ogasawara Islands in Japan, Nanwan Bay in Taiwan, and Masthead Island in northern Australia) from 1950 to 2017. From these data, anomalous radiocarbon signals observed in Ishigaki Island data during 1955 ($n = 18$) were excluded from analysis to avoid bias in the age estimation model. The posterior predictive chronology captured the rapid post-bomb increase in marine $F^{14}C$ followed by the subsequent decline (Fig. 2). The model predicted a peak in 1975, with a peak $F^{14}C$ value of 1.165 (Fig. 2).

Radiocarbon measurement and age estimation

Age estimation was performed on 12 adult turtles using lens $F^{14}C$ values calibrated against the regional reference chronology (Fig. 3, Table 1). When the innermost eye lens section exhibited a higher $F^{14}C$ value than the second (or third) innermost section, we interpreted the individual as having hatched after the atmospheric bomb peak. In theory, an innermost layer could show higher $F^{14}C$ even if the turtle was born before the bomb peak if the second (or third) innermost section formed after the peak and had lower $F^{14}C$ than the innermost layer, which would in turn require a substantial temporal gap between the formation of these layers so that the second (or third) section lay on the post-peak decline. However, this scenario is unlikely, as these second- and third-innermost sections were adjacent to the core, and such age estimates under this assumption would imply implausibly low growth rates.

For the three samples with large innermost sections, we assumed the core sample included some outer material formed several years after hatching. The sample was assigned a “core size” of half the measured mass of the innermost section (7.25, 8.4, or 9.25 mg), and 7.6 years were added to the estimated age, as the mean age observed for samples of similar eye lens size (6.6–9.7 mg, $n = 4$) was 7.6 ± 5.5 years. After this adjustment, estimated ages (median) ranged from 34.9 to 45.6 years for females (mean: 39.0 ± 3.4 years) and from 29.5 to 48.1 years for males (mean: 39.0 ± 6.6 years, Table 1).

Growth curve

Based on 48 paired measurements of ELW and SCL, an allometric relationship was established (Fig. 4). The raw relationship was described by: $ELW = 0.054 \times (SCL)^{1.57}$ ($R^2 = 0.94$).

Downloaded from academic.oup.com/icesjms/article/83/10/fsag208/9004402 by guest on 01 November 2026

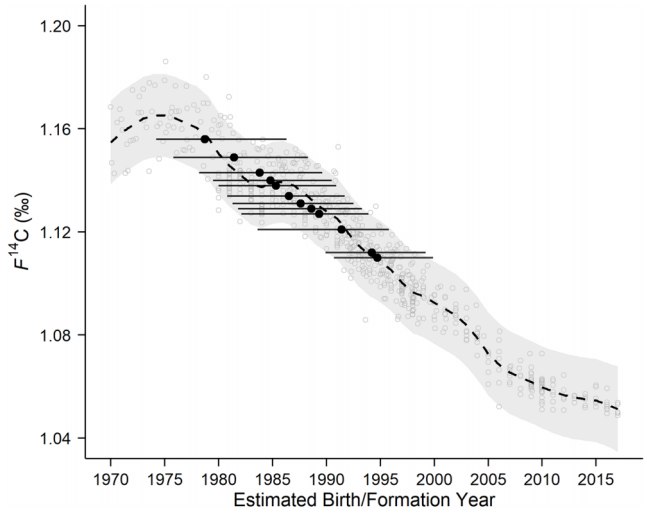


Figure 3 Estimated birth years for the 12 individual sea turtles. Black filled circles and horizontal solid lines indicate the estimated posterior medians and 95% credible intervals for each sea turtle, respectively. These points and lines are overlaid on a magnified section of the reference chronology shown in Figure 2. The background dashed line and shaded band represent the predictive median and 95% prediction interval of the regional $F^{14}C$ reference curve, respectively. Gray open circles denote the observed coral $F^{14}C$ values within the corresponding period. Note that all individuals were collected within a narrow time window in March–April 2024. The lifespan of each individual was calculated from the difference between this collection timing (defined as 2024.2–2024.3 in decimal years) and the estimated birth year (the black filled circle).

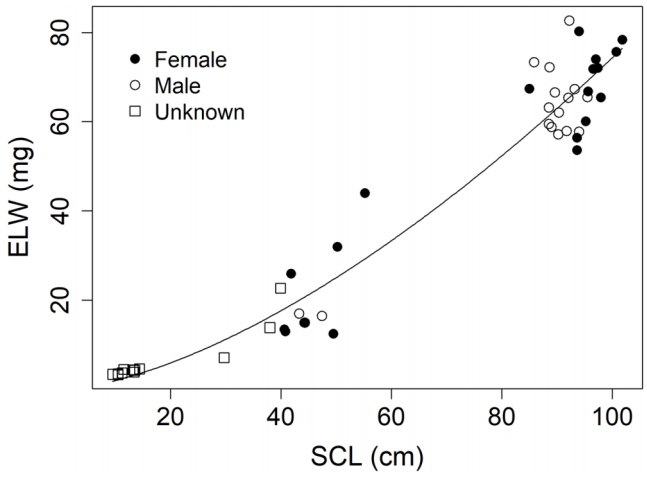


Figure 4 Relationship between straight carapace length (SCL) and eye lens weight (ELW) in 48 individuals. The fitted allometric regression is shown.

For estimation purposes, SCL can be calculated from ELW using:

$$\mathrm{SCL} = (\mathrm{ELW}/0.054)^{0.637}$$

Using the relationship between eye lens size and body size, growth curves were reconstructed for three individuals with multiple $F^{14}C$ measurements (Fig. 5). In all but one section, $F^{14}C$ values decreased toward the outer layers. Growth trajectories were well fitted by the Von Bertalanffy growth model, and estimated SCL near maximum lifespan (age ≈ 60) ranged from 108 to 123 cm. When growth rates were calculated from the model as a function of body size, they were 2.7–5.0 cm/year and 1.7–1.8 cm/year at an SCL of 20 cm and 80 cm, respectively (Supplementary Fig. S1).

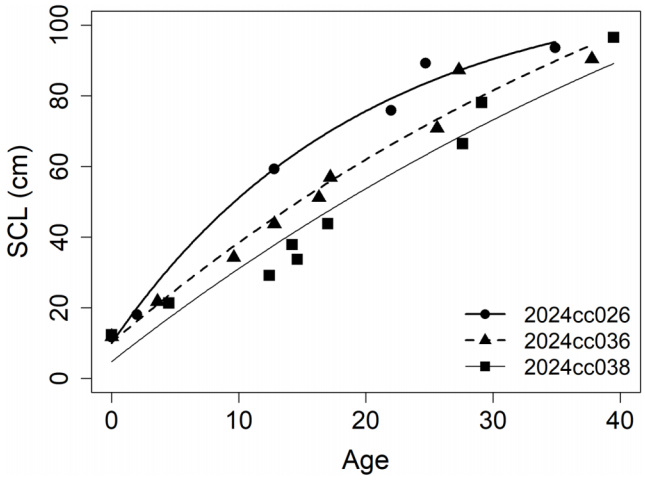


Figure 5 Growth trajectories reconstructed from radiocarbon measurements of multiple eye lens sections. Growth of two females (2024cc026 and 2024cc038) and one male (2024cc036) is shown. Estimated body sizes at each section are plotted against the estimated age, and fitted von Bertalanffy growth curves are superimposed.

Discussion

Radiocarbon analysis of the central eye lens sections enabled age estimation of wild *C. mydas*, and sequential measurements toward the outer eye lens sections allowed reconstruction of growth trajectories. This study demonstrates that reptilian eye lenses can be used for time-series stable isotope analysis, establishing that the lens provides a metabolically inert, chronologically layered structure suitable for retrospective ecological and life-history reconstruction.

Age estimation provided fundamental ecological information for green turtles, such as maturation age. Green turtles that migrate to the Ogasawara Islands are sexually mature individuals returning to their natal waters to breed. All females exhibited corpora albicantia in their ovaries, confirming they were reproductively experienced. This indicates that each female turtle visited Ogasawara at least once before sampling (Kamezaki 2012). Female green turtles exhibit reproductive intervals of 3–4 years (Abe et al. 2003, Balazs et al. 2015). Therefore, the youngest females must have initiated reproduction 3–4 years before the ages determined here. Male green turtles exhibit higher breeding frequencies, returning to breeding grounds roughly two times as often as females (Hays et al. 2022). Our results yielded youngest ages of 35 and 30 years for females and males, respectively, suggesting they reach sexual maturity by 31 and 28 years of age at the latest, respectively. This estimate lies within the range of previously reported maturation ages for this species in the Pacific, such as 19–40 years

Downloaded from academic.oup.com/icesjms/article/83/10/fsag208/9004402 by guest on 01 November 2026

(Zug et al. 2002), 25–50 years (Chaloupka et al. 2004), and 14–39 years (Turner Tomaszewicz et al. 2022). Therefore, our result can be considered reasonably reliable and consistent with these studies. However, estimates of age at sexual maturity in sea turtles vary widely (Sanchez et al. 2023), with even higher ages reported (over 40 years, Van Houtan et al. 2014). Further accumulation of data is therefore required to refine these estimates.

The other key information obtained was longevity. The oldest individuals identified were a 46-year-old female and 48-year-old male. As green turtles reproduce throughout their lives (Parham and Zug 1997), it is reasonable to assume that the oldest nesting individuals represent the approximate maximum lifespan of the population. Although a larger sample size is required to refine longevity estimates, the data indicate that green turtles nesting in the Ogasawara Islands live for at least approximately 47 years. This estimate is slightly less than longevity estimates from genomic approaches in other sea turtle species and shorter than the reported case of a 75-year-old green turtle (Mayne et al. 2020). According to data by Humburg and Balazs (2014), 82% of all recaptures ($n = 2138$) had recapture durations of ≤ 15 years, comparable to the interval between estimated sexual maturity and maximum ages observed in this study. When considered in this context, the longevity estimates derived here appear consistent with long-term mark–recapture patterns. Our results suggest that, despite a potentially longer maximum lifespan, the realized lifespan of most green turtles in the Ogasawara wild population is around 47 years. Sea turtles, known for exceptional longevity and wide-ranging migratory behavior, pose challenges for reliable longevity estimation using conventional methods such as mark–recapture (Casale et al. 2007). This approach offers a framework for overcoming these limitations, providing opportunities to elucidate life-history traits that remained intractable for such long-lived and migratory organisms.

Sources of uncertainty in our age estimates would stem from marine radiocarbon reference data. Post-bomb marine radiocarbon concentrations display marked spatial heterogeneity in the timing and height of the bomb peak (Grammer et al. 2015, Christiansen et al. 2016), introducing substantial uncertainty into age estimates from $F^{14}C$ of migratory animals such as green turtles. Atmospheric pre-bomb peaks mainly fluctuate by latitude (Reimer et al. 2004, Dutta 2016), whereas oceanic radiocarbon records show variation in longitudinal direction, as documented in the eastern South Pacific from Fiji to Easter Island (Andrews et al. 2021). Therefore, obtaining $\Delta^{14}C$ reference data covering a broad range of the target organism's migratory habitat is essential for radiocarbon-based age assessments. In green turtles, the lens nucleus forms before hatching and likely retains the $F^{14}C$ signature of the maternal foraging area inhabited before nesting. In this regard, our age estimation is reliable because our reference $\Delta^{14}C$ data encompass typical foraging habitats of the green turtle population in the western North Pacific, and coral $\Delta^{14}C$ time series exhibited no clear latitudinal differentiation from Okinawa to northern Australia. Our reference $\Delta^{14}C$ data did not cover some northern potential foraging habitats, such as the Tohoku coast, Japan. However, the Tohoku coast is a summer-restricted foraging ground used only by juvenile to sub-adult individuals (Fukuoka et al. 2019). Adult females before nesting do not forage in this region, and potential influence on our age estimates is considered negligible.

Another source of uncertainty in age estimation arises from potential contamination of late-formed lens material, reflecting an inherent limitation of the eye-lens dissection procedure. Sea turtle eye lenses are oblate spheroids and extremely fragile; thus, they cannot be separated into concentric chronological layers similar to fish eye lenses (Patterson III et al. 2021, Chu et al. 2025). Therefore, it is necessary to scrape sections while maintaining a spheroidal shape. However, this procedure does not guarantee sections correspond to a single temporal layer, and materials formed later may be contaminated. The innermost portion used for age estimation was particularly fragile, making it difficult to reach the nucleus while maintaining its shape. Consequently, it is possible that some material formed after hatching was incorporated into age determination samples. If outer material was included, the measured $F^{14}C$ would be lower for individuals hatched after the bomb peak, leading to age underestimation. However, samples with oversized innermost layers were corrected as mentioned above, and for remaining individuals, we reduced innermost samples to match hatchling lens size (Table 1). Therefore, slight underestimation cannot be ruled out, but any effect is likely minor. To reliably implement this approach in future studies, lens sectioning must be performed with exceptional care.

Building on the reliability of this age estimation method, using the entire lens allows analyses beyond age estimation. By combining sequential lens sectioning, age determination for each section, and body size estimation at formation time, we reconstructed individual growth histories of wild sea turtles. The estimated SCL at expected maximum lifespan from these growth curves (108–123 cm) matched with the maximum SCL of 116 cm reported for green turtles in the Pacific Ocean (Hirth 1971). The calculated growth rates (1.7–1.8 cm/year at SCL = 80 cm) also fall within ranges reported from mark–recapture studies (ca. 1.5 cm/year; Limpus and Chaloupka 1997), and 1.5–3.5 cm/year; Patricio et al. 2014), and align with skeletochronology results (1.3 cm/year; Zug et al. 2002, and 2.6 cm/year; Goshe et al. 2010). These findings support the validity of the present approach. This method enables individual-level reconstruction of long-term growth histories from early life stages, previously difficult for sea turtles.

$F^{14}C$ chronologies of eye lenses yield robust absolute age estimates for sea turtles, but require lethal sampling, precluding use in living or legally protected individuals (Zhang et al. 2024). A promising solution is calibrating non-lethal biomarkers, particularly DNA methylation-based methods (De Paoli-Iseppi et al. 2017), against radiocarbon ages from deceased specimens. Analyzing radiocarbon and DNA methylation patterns in the same individuals would provide wild-caught reference data that epigenetic clocks currently lack. Eye lens radiocarbon ages can also serve as an independent yardstick for validating other age proxies, such as skeletochronology of bone or scute tissues (Zug et al. 1986, Bjorndal et al. 1998). Establishing a reliable framework for absolute age determination through these validations will improve estimates of growth rates and life-history schedules. Furthermore, sequential eye lens isotope analysis, combining bomb ^{14}C dating with stable isotope measurements, can

Downloaded from academic.oup.com/icesjms/article/83/10/fsag208/9004402 by guest on 01 November 2026

elucidate timing, and location of habitat shifts (Matsubayashi et al. 2020, Sakamoto et al. 2023). These methodological advances will provide wildlife biologists and conservation practitioners with precise means to quantify population age structure, monitor demographic trends, and evaluate ecological conditions, strengthening evidence-based management of sea turtle populations.

Acknowledgements

We are grateful to the sea turtle fishers on Chichi-jima Island, turtle buyers, and fishers on Mikura Island for their cooperation in sample collection. We sincerely thank Chiyo Kitayama, Nanako Shimizu, and all the staff of Everlasting Nature for introducing sampling sites, providing generous field support, and offering valuable advice throughout the sampling. We appreciate the assistance of Hirotaka Tajima, Hideaki Nishizawa, Junichi Okuyama, and Yoshimitsu Tsukakoshi in collecting and providing samples from Kume-jima Island, as well as Takehiro Mitsuguchi for providing $\Delta\,^{14}C$ data from Okinawa.

Author contributions

Moe Kaida (Data curation [equal], Investigation [lead], Writing—original draft [equal], Writing—review & editing [supporting]), Jun Matsubayashi (Conceptualization [equal], Formal Analysis [equal], Funding acquisition [equal], Methodology [lead], Resources [equal], Software [lead], Validation [equal], Writing—original draft [equal], Writing—review & editing [equal]), Satomi Kondo (Investigation [supporting], Resources [equal], Writing – review & editing [supporting]), Ichiro Tayasu (Investigation [supporting], Resources [equal], Writing—review & editing [supporting]), and Noriko Iwai (Conceptualization [equal], Data curation [lead], Formal Analysis [supporting], Funding acquisition [equal], Project administration [lead], Resources [supporting], Supervision [equal], Visualization [lead], Writing—original draft [equal], Writing—review & editing [equal])

Supplementary material

Supplementary material is available at *ICES Journal of Marine Science* online.

Conflicts of interest

None declared.

Funding

This research has received the financial support from JSPS KAKENHI Grant Numbers JP20KK0165, JP21H03579, JP21H04784, JP21K05684, JP22H05028, JP22K19197, and JP25K03305.

Data availability

The data supporting this study have been deposited in Zenodo at: https://doi.org/10.5281/zenodo.20276636

References

Abe O, Shibuno T, Takada Y *et al.* Nesting populations of sea turtle in Ishigaki Island, Okinawa. *Proceedings on the 4th SEASTAR2000 Workshop* 2003;**40**.

Andrews AH, Barnett BK, Allman RJ *et al.* Great longevity of speckled hind (*Epinephelus drummondhayi*), a deep-water grouper, with novel use of postbomb radiocarbon dating in the Gulf of Mexico. *Canadian J Fish Aquat Sci* 2013;**70**:1131–40. https://doi.org/10.1139/cjfas-2012-0537

Andrews AH, Choat JH, Hamilton RJ *et al.* Refined bomb radiocarbon dating of two iconic fishes of the Great Barrier Reef. *Mar Freshw Res* 2014;**66**:305–16. https://doi.org/10.1071/mf14086

Andrews AH, Prouty NG, Cheriton OM. Bomb-produced radiocarbon across the South Pacific Gyre—a new record from American Samoa with utility for fisheries science. *Radiocarbon* 2021;**63**:1591–605. https://doi.org/10.1017/rdc.2021.51

Avens L, Goshe LR, Coggins L *et al.* Age and size at maturation- and adult-stage duration for Loggerhead Sea Turtles in the Western North Atlantic. *Mar Biol* 2015;**162**:1749–67. https://doi.org/10.1007/s00227-015-2705-x

Avens L, Ramirez MD, Goshe LR *et al.* Hawksbill sea turtle life-stage durations, somatic growth patterns, and age at maturation. *Endang Species Res* 2021;**45**:127–45. https://doi.org/10.3354/esr01123

Balazs GH, Van Houtan KS, Hargrove SA *et al.* A review of the demographic features of Hawaiian geen turtles (*Chelonia mydas*). *Chelonian Conserv Biol* 2015;**14**:119–29. https://doi.org/10.2744/CCB-1172.1

Bjorndal KA, Bolten AB, Bennett RA *et al.* Age and growth in sea turtles: limitations of skeletochronology for demographic studies. *Copeia* 1998;**1998**:23. https://doi.org/10.2307/1447698

Casale P, Mazaris AD, Freggi D *et al.* Survival probabilities of loggerhead sea turtles (*Caretta caretta*) estimated from capture-mark-recapture data in the Mediterranean Sea. *Sci Mar* 2007;**71**:365–72. https://doi.org/10.3989/scimar.2007.71n2365

Catalano MJ, Allen MS. A size- and age-structured model to estimate fish recruitment, growth, mortality, and gear selectivity. *Fish Res* 2010;**105**:38–45. https://doi.org/10.1016/j.fishres.2010.03.002

Chaloupka M, Limpus C, Miller J. Green turtle somatic growth dynamics in a spatially disjunct Great Barrier Reef metapopulation. *Coral Reefs* 2004;**23**:325–35. https://doi.org/10.1007/s00338-004-0387-9

Chen X, Liu B, Fang Z. Age and growth of fish. In: *Biology of Fishery Resources*. 71. Chen X, Liu B (eds). Singapore: Springer Nature Singapore, 2022. https://doi.org/10.1007/978-981-16-6948-4 10.1007/978-981-16-6948-4_4

Christiansen HM, Campana SE, Fisk AT *et al.* Using bomb radiocarbon to estimate age and growth of the white shark, *Carcharodon carcharias*, from the southwestern Indian Ocean. *Mar Biol* 2016;**163**:144. https://doi.org/10.1007/s00227-016-2916-9

Downloaded from academic.oup.com/icesjms/article/83/10/fsag208/9004402 by guest on 01 November 2026

Chu A, Li DA, Bell-Tilcock M *et al.* Enhancing reproducibility in stable isotope analysis (SIA) of fish eye lenses: a comparison between lamina number and diameter. *PLoS One* 2025;**20**:e0326345. https://doi.org/10.1371/journal.pone.0326345

De Paoli-Iseppi R, Deagle BE, McMahon CR *et al.* Measuring animal age with DNA methylation: from humans to wild animals. *Front Genet* 2017;**8**:106. https://doi.org/10.3389/fgene.2017.00106

Dolfo V, Gaspar C, Bourjea J *et al.* Population genetic structure and mixed stock analysis of the green sea turtle, *Chelonia mydas*, reveal reproductive isolation in French Polynesia. *Front Mar Sci* 2023;**10**:1201384. https://doi.org/10.3389/fmars.2023.1201384

Dutta K. Sun, ocean, nuclear bombs, and fossil fuels: radiocarbon variations and implications for high-resolution dating. *Annu Rev Earth Planet Sci* 2016;**44**:239–75. https://doi.org/10.1146/annurev-earth-060115-012333

Eglinton TI, Graven HD, Raymond PA *et al.* Making the case for an international decade of radiocarbon. *Philos Trans R Soc A* 2023;**381**:20230081. https://doi.org/10.1098/rsta.2023.0081

Fisheries Agency of Japan. (ed.) *Basic Data on Rare Wild Aquatic Organisms in Japan [in Japanese]*. Tokyo:Fisheries Agency and Japan Fisheries Resource Conservation Association, 1994.

Fukuoka T, Narazaki T, Kinoshita C *et al.* Diverse foraging habits of juvenile green turtles (*Chelonia mydas*) in a summer-restricted foraging habitat in the northwest Pacific Ocean. *Mar Biol* 2019;**166**:25. https://doi.org/10.1007/s00227-019-3481-9

Goshe LR, Avens L, Scharf FS *et al.* Estimation of age at maturation and growth of Atlantic green turtles (*Chelonia mydas*) using skeletochronology. *Mar Biol* 2010;**157**:1725–40. https://doi.org/10.1007/s00227-010-1446-0

Grammer GL, Fallon SJ, Izzo C *et al.* Investigating bomb radiocarbon transport in the southern Pacific Ocean with otolith radiocarbon. *Earth Planet Sci Lett* 2015;**424**:59–68. https://doi.org/10.1016/j.epsl.2015.05.008

Hasegawa EA, Matsubayashi J, Tayasu I *et al.* Isotope analysis of birds' eye lens provides early-life information. *Prog Earth Planet Sci* 2025;**12**:9. https://doi.org/10.1186/s40645-024-00677-0

Hays GC, Shimada T, Schofield G. A review of how the biology of male sea turtles may help mitigate female-biased hatchling sex ratio skews in a warming climate. *Mar Biol* 2022;**169**:89. https://doi.org/10.1007/s00227-022-04074-3

Hirabayashi S, Yokoyama Y, Suzuki A *et al.* Multidecadal oceanographic changes in the western Pacific detected through high-resolution bomb-derived radiocarbon measurements on corals. *Geochem Geophys Geosyst* 2017;**18**:1608–17. https://doi.org/10.1002/2017GC006854

Hirth HF. Synopsis of biological data on the green turtle *Chelonia mydas* (Linnaeus 1758). *FAO Fish Synop* 1971;**85**:1–120.

Hixon MA, Johnson DW, Sogard SM. BOFFFFs: on the importance of conserving old-growth age structure in fishery populations. *ICES J Mar Sci* 2014;**71**:2171–85. https://doi.org/10.1093/icesjms/fst200

Horwitz J. Alpha-crystallin. *Exp Eye Res* 2003;**76**:145–53. https://doi.org/10.1016/S0014-4835(02)00278-6

Humburg IN, Balazs GH. *Forty Years of Research: Recovery Records of Green Turtles Observed or Originally Tagged at French Frigate Shoals in the Northwestern Hawaiian Islands, 1973-2013*. Honolulu: U.S. Dep. Commer., NOAA Tech. Memo., NMFS-PIFSC-40, 2014. https://doi.org/10.7289/V5DV1GTC

Jensen MP, LaCasella EL, Kobayashi DR *et al.* Expanding the boundaries: regional connectivity in green turtle (*Chelonia mydas*) populations across Micronesia. *Front Mar Sci* 2025;**12**:1558792. https://doi.org/10.3389/fmars.2025.1558792

Kameda K, Ishihara T. Gut contents analysis of green turtles (*Chelonia mydas*) in Japan. *Umigame Newslett Japan* 2009;**81**:17–23.

Kamezaki N. *Natural History of Sea Turtles in Japan*. Tokyo: University of Tokyo Press, 2012.

Kitagawa H, Masuzawa T, Makamura T *et al.* A batch preparation method for graphite targets with low background for AMS 14C measurements. *Radiocarbon* 1993;**35**:295–300. https://doi.org/10.1017/s0033822200064973

Konishi K, Tanaka T, Sakanoue M. Secular variation of radiocarbon concentration in seawater: a sclerochronological approach. In: Gomez ED, Birkeland CE, Buddemeier RW (eds), *The Reef and Man: Proceedings of the Fourth International Coral Reef Symposium*. Manila, Philippines: University of the Philippines, 1981,181–5.

Leifsdóttir RR, Campana SE. Species independence of eye lens dimensions in teleosts and elasmobranchs. *PLoS One* 2023;**18**:e0286388. https://doi.org/10.1371/journal.pone.0286388

Limpus C, Chaloupka M. Nonparametric regression modelling of green sea turtle growth rates (southern Great Barrier Reef). *Mar Ecol Prog Ser* 1997;**149**:23–34. https://doi.org/10.3354/meps149023

Matsubayashi J, Osada Y, Kimura K *et al.* Fine-scale reconstruction of pelagic fish migration by iso-logging of eye lens. *Methods Ecol Evol* 2026;**17**:77–84. https://doi.org/10.1111/2041-210x.70201

Matsubayashi J, Osada Y, Tadokoro K *et al.* Tracking long-distance migration of marine fishes using compound-specific stable isotope analysis of amino acids. *Ecol Lett* 2020;**23**:881–90. https://doi.org/10.1111/ele.13496

Matsubayashi J, Tayasu I. Collagen turnover and isotopic records in cortical bone. *J Archaeological Sci* 2019;**106**:37–44. https://doi.org/10.1016/j.jas.2019.03.010

Mayne B, Tucker AD, Berry O *et al.* Lifespan estimation in marine turtles using genomic promoter CpG density. *PLoS One* 2020;**15**:e0236888. https://doi.org/10.1371/journal.pone.0236888

Medetian D, Miaud C. Age and growth rate estimated by skeletochronology in loggerhead sea turtles from French Mediterranean waters. *Amphibia-Reptilia* 2024;**45**:415–26. https://doi.org/10.1163/15685381-bja10197

Mitsuguchi T, Hirota M *et al.* Paleo Labo AMS Dating Group *et al.* Post-bomb coral Δ^{14}C record from Iki Island, Japan: possible evidence of oceanographic conditions on the northern East China Sea shelf. *Geo-Mar Lett* 2016;**36**:371–7. https://doi.org/10.1007/s00367-016-0456-4

Mitsuguchi T, Kitagawa H, Matsumoto E *et al.* High-resolution ^{14}C analyses of annually-banded coral skeletons from Ishigaki Island, Japan: implications for oceanography. *Nucl Instrum Methods Phys Res Sect B* 2004;**223-224**:455–9. https://doi.org/10.1016/j.nimb.2004.04.086

Downloaded from academic.oup.com/icesjms/article/83/10/fsag208/9004402 by guest on 01 November 2026

Miura K, Matsubayashi J, Yoshimizu C *et al.* A novel method for fine-scale retrospective isotope analysis in mammals using eye lenses. *Ecosphere* 2025;**16**:e70276. https://doi.org/10.1002/ecs2.70276

Mohamed A, Augusteyn RC. Human lens weights with increasing age. *Mol Vis* 2018;**24**:867–74.

Morimoto M, Kitagawa H, Shibata Y *et al.* Seasonal radiocarbon variation of surface seawater recorded in a coral from Kikai Island, subtropical northwestern Pacific. *radiocarb* 2004;**46**:643–8. https://doi.org/10.1017/s0033822200035694

Mortimer JA. Feeding ecology of sea turtles. In: Bjorndal KA (ed.), *Biology and Conservation of Sea Turtles*. Washington, D.C.: Smithsonian Institution Press, 1982,103–9.

Nielsen J, Hedeholm RB, Heinemeier J *et al.* Eye lens radiocarbon reveals centuries of longevity in the Greenland shark (*Somniosus microcephalus*). *Science* 2016;**353**:702–4. https://doi.org/10.1126/science.aaf1703

Nishizawa H, Naito Y, Suganuma H *et al.* Composition of green turtle feeding aggregations along the Japanese archipelago: implications for changes in composition with current flow. *Mar Biol* 2013;**160**:2671–85. https://doi.org/10.1007/s00227-013-2261-1

Nishizawa H, Narazaki T, Fukuoka T *et al.* Juvenile green turtles on the northern edge of their range: mtDNA evidence of long-distance westward dispersals in the northern Pacific Ocean. *Endangered Species Res* 2014;**24**:171–9. https://doi.org/10.3354/esr00592

Parham JF, Zug GR. Age and growth of loggerhead sea turtles (*Caretta caretta*) of coastal Georgia: an assessment of skeletochronological age-estimates. *Bull. Mar. Sci.* 1997;**61**:287.

Patricio A, Diez C, Van Dam R. Spatial and temporal variability of immature green turtle abundance and somatic growth in Puerto Rico. *Endang Species Res* 2014;**23**:51–62. https://doi.org/10.3354/esr00554

Patterson WF, Barnett BK, TinHan TC *et al.* Eye lens $\Delta^{14}C$ validates otolith-derived age estimates of Gulf of Mexico reef fishes. *Can J Fish Aquat Sci* 2021;**78**:13–7. https://doi.org/10.1139/cjfas-2020-0237

Ramos RD, Goodkin NF, Druffel ERM *et al.* Interannual coral $\Delta^{14}C$ records of surface water exchange across the Luzon strait. *J Geophys Res Oceans* 2019;**124**:491–505. https://doi.org/10.1029/2018JC014735

R Core Team. *R: a Language and Environment for Statistical Computing*. R Foundation for Statistical Computing. 2025.https://www.r-project.org/ (7 July 2026, date last accessed).

Reimer PJ, Brown TA, Reimer RW. Discussion: reporting and calibration of post-bomb ^{14}C data. *Radiocarbon* 2004;**46**:1299–304. https://doi.org/10.1017/s0033822200033154

Saito-Kokubu Y, Mitsuguchi T, Watanabe T *et al.* Preliminary test of the EA-AGE3 system for ^{14}C measurement of $CaCO_3$ samples and coral-based estimation of marine reservoir correction in the Ogasawara Islands, Northwestern Subtropical Pacific. *Radiocarbon* 2019;**61**:1593–601. https://doi.org/10.1017/rdc.2019.69

Sakamoto T, Horii S, Kodama T *et al.* Stable isotopes in eye lenses reveal migration and mixing patterns of diamond squid in the western North Pacific and its marginal seas. *ICES J Mar Sci* 2023;**80**:2313–28. https://doi.org/10.1093/icesjms/fsad145

Sanchez CL, Bunbury N, Mortimer JA *et al.* Growth rate and projected age at sexual maturity for immature hawksbill turtles and green turtles foraging in the remote marine protected area of Aldabra Atoll, Seychelles. *Mar Biol* 2023;**170**:49. https://doi.org/10.1007/s00227-023-04197-1

Seminoff JA. *IUCN Red List Global Status Assessment: green Turtle (Chelonia mydas)*. Marine Turtle Specialist Group, Species Survival Commission, The World Conservation Union (IUCN), 2002. https://www.widecast.org/Resources/Docs/MTSG_Assessment_CM_2002.pdf (9 October 2026 date last accessed).

Shervette VR, Rivera Hernández JM, Van Sant SB *et al.* Bomb radiocarbon in otoliths and eye lenses of reef fishes from Atlantic waters of the southeastern U.S. *Environ Biol Fis* 2025;**108**:1131–49. https://doi.org/10.1007/s10641-025-01713-8

Shiga A, Matsubayashi J, Ogawa NO *et al.* Assessing the applicability of sequential eye lens stable isotope analysis for reconstructing dietary histories in amphibians. *Limnol Oceanogr Methods* 2025;**23**:336–45. https://doi.org/10.1002/lom3.10689

Singaram G, Cheung N, Yip B *et al.* Medaka fish exhibits longevity gender gap, a natural drop in estrogen and telomere shortening during aging: a unique model for studying sex-dependent longevity. *Front Zool* 2013;**10**:78. https://doi.org/10.1186/1742-9994-10-78

Smoliński S, Gutkowska J. Otolith biochronology for the long-term reconstruction of growth and stock dynamics of fish. *Rev Fish Biol Fish* 2024;**34**:405–19. https://doi.org/10.1007/s11160-023-09820-4

Suetsugu K, Matsubayashi J, Tayasu I. Some mycoheterotrophic orchids depend on carbon from dead wood: novel evidence from a radiocarbon approach. *New Phytologist* 2020;**227**:1519–29. https://doi.org/10.1111/nph.16409

Tsikliras AC, Stergiou KI. Age at maturity of Mediterranean marine fishes. *Mediterranean Mar Sci* 2015;**16**:5. https://doi.org/10.12681/mms.659

Turner Tomaszewicz CN, Avens L, Seminoff JA *et al.* Age-specific growth and maturity estimates for the flatback sea turtle (*Natator depressus*) by skeletochronology. *PLoS One* 2022;**17**:e0271048. https://doi.org/10.1371/journal.pone.0271048

Usategui-Martín A, Valverde RA, Ostiategui-Francia P *et al.* First skeletochronological analysis on loggerhead yearlings (*Caretta caretta*) in the Canary Islands. *Mar Biol* 2023;**170**:95. https://doi.org/10.1007/s00227-023-04239-8

van Buskirk J, Crowder LB. Life-history variation in marine turtles. *Copeia* 1994;**1994**:66. https://doi.org/10.2307/1446672

Van Houtan KS, Andrews AH, Jones TT *et al.* Time in tortoiseshell: a bomb radiocarbon-validated chronology in sea turtle scutes. *Proc R Soc B Biol Sci* 2016;**283**:20152220. https://doi.org/10.1098/rspb.2015.2220

Van Houtan KS, Hargrove SK, Balazs GH. Modeling sea turtle maturity age from partial life history records. *Pac Sci* 2014;**68**:465–77. https://doi.org/10.2984/68.4.2

Wallace AA, Hollander DJ, Peebles EB. Stable isotopes in fish eye lenses as potential recorders of trophic and geographic history. *PLoS One* 2014;**9**:e108935. https://doi.org/10.1371/journal.pone.0108935

Wu Y, Fallon SJ, Cantin NE *et al.* Surface ocean radiocarbon from a porites coral record in the Great Barrier Reef: 1945–2017. *Radiocarbon* 2021;**63**:1193–203. https://doi.org/10.1017/rdc.2020.141

Downloaded from academic.oup.com/icesjms/article/83/10/fsag208/9004402 by guest on 01 November 2026

Zeng Y, Yokoyama Y, Hirabayashi S *et al.* Anthropocene north western Pacific oceanography recorded as seasonal-resolution radiocarbon in coral from Kikai Island, Japan. *Global Biogeochem Cycles* 2024;**38**:e2023GB007927. https://doi.org/10.1029/2023GB007927

Zhang Y, Bi J, Ning Y *et al.* Methodology advances in vertebrate age estimation. *Animals* 2024;**14**:343. https://doi.org/10.3390/ani14020343

Zug GR, Balazs GH, Wetherall JA *et al.* Age and growth of Hawaiian green seaturtles (*Chelonia mydas*): an analysis based on skeletochronology. *Fish Bull* 2002;**100**:117.

Zug GR, Wynn AH, Ruckdeschel C. *Age Determination of Loggerhead Sea Turtles, Caretta caretta, by Incremental Growth Marks in the Skeleton*. Washington:Smithsonian Institution Press, 1986. https://doi.org/10.5479/si.00810282.427

Handling editor: Allen Andrews

Downloaded from academic.oup.com/icesjms/article/83/10/fsag208/9004402 by guest on 01 November 2026

Received: 4 June 2026. **Revised:** 30 September 2026. **Accepted:** 1 October 2026

© The Author(s) 2026. Published by Oxford University Press on behalf of International Council for the Exploration of the Sea. This is an Open Access article distributed under the terms of the Creative Commons Attribution License (https://creativecommons.org/licenses/by/4.0/), which permits unrestricted reuse, distribution, and reproduction in any medium, provided the original work is properly cited.